JACS
JOURNAL OF THE AMERICAN CHEMICAL SOCIETY
Article
pubs.acs.org/JACS

Solid-Phase Polarization Matrixes for Dynamic Nuclear Polarization from Homogeneously Distributed Radicals in Mesostructured Hybrid Silica Materials

David Gajan,[†,‡,⊥] Martin Schwarzwälder,[†,⊥] Matthew P. Conley,[†] Wolfram R. Grüning,[†] Aaron J. Rossini,[‡] Alexandre Zagdoun,[‡] Moreno Lelli,[‡] Maxim Yulikov,[†] Gunnar Jeschke,[†] Claire Sauvée,[§] Olivier Ouari,[§] Paul Tordo,[§] Laurent Veyre,[∥] Anne Lesage,[‡] Chloé Thieuleux,*[,∥] Lyndon Emsley,*[,‡] and Christophe Copéret*[,†]

[†]Department of Chemistry, ETH Zürich, CH-8093 Zürich, Switzerland
[‡]Centre de RMN à Très Hauts Champs, Université de Lyon (CNRS/ENS Lyon/UCB Lyon 1), 69100 Villeurbanne, France
[§]Institut de Chimie Radicalaire (ICR) UMR 7273, Aix-Marseille Université, CNRS, 13397 Marseilles Cedex 20, France
[∥]Institut de Chimie de Lyon, C2P2, CPE Lyon, Université de Lyon, 69100 Villeurbanne, France

Supporting Information

ABSTRACT: Mesoporous hybrid silica−organic materials containing homogeneously distributed stable mono- or dinitroxide radicals covalently bound to the silica surface were developed as polarization matrixes for solid-state dynamic nuclear polarization (DNP) NMR experiments. For TEMPO-containing materials impregnated with water or 1,1,2,2-tetrachloroethane, enhancement factors of up to 36 were obtained at ∼100 K and 9.4 T without the need for a glass-forming additive. We show that the homogeneous radical distribution and the subtle balance between the concentration of radical in the material and the fraction of radicals at a sufficient inter-radical distance to promote the cross-effect are the main determinants for the DNP enhancements we obtain. The material, as well as an analogue containing the poorly soluble biradical bTUrea, is used as a polarizing matrix for DNP NMR experiments of solutions containing alanine and pyruvic acid. The analyte is separated from the polarization matrix by simple filtration.

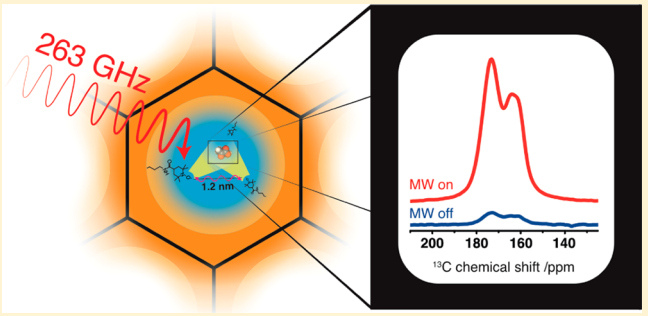

INTRODUCTION

Nuclear magnetic resonance (NMR) is the most widely used and information-rich technique currently available to the analytical sciences. NMR provides a detailed atomic-level probe, which has led to a wide range of applications unique to this technique. NMR has broad applications in chemistry, materials sciences, structural biology and the analysis of biomedical samples. However, the Achilles' heel of NMR is the low sensitivity of the method that prevents its use in many applications such as sensing or molecular imaging.

There is intense current interest in enhancing NMR sensitivity, and several methods are being explored, with dynamic nuclear polarization (DNP)[1,2] being of particular interest. In DNP, polarization is transferred from unpaired electrons to nuclei, usually at low temperature (from 1 to 100 K), leading to NMR polarization enhancements of up to 4 orders of magnitude as compared to conventional room temperature NMR experiments. If this method could be generalized, it could make NMR experiments possible in toxicological and environmental sensing applications, or even as a tracer method for molecular imaging in vivo.[3−13]

So far low-temperature DNP has mostly been applied to enhance the NMR signals of frozen solutions containing exogenous radicals.[4,6−8,11−19] The polarized frozen solutions can then be rapidly thawed and used as a contrast agent in imaging or in spectroscopy (dissolution DNP).[3,4,6−13] These frozen solutions can also be studied in situ at low temperature by magic angle spinning solid-state NMR.[14−19] The latter approach has been employed extensively to study biomolecules in frozen solutions and membranes.[20−28] We have recently shown how materials that have been impregnated with radical solution can be studied using DNP,[29] with applications to surface science and catalysis[30−33] or to traditional solid-state NMR of microcrystalline powders.[34]

The exogenous polarization sources are almost always stable organic radicals, either nitroxides such as 2,2,6,6-tetramethylpiperidine-1-oxyl (TEMPO), carbon-centered radicals (e.g., trityl, BDPA, OX063),[35,36] or biradicals optimized for cross-effect DNP.[37] To ensure homogeneous polarization, the radical in

Received: June 10, 2013
Published: August 26, 2013

   dx.doi.org/10.1021/ja405822h | J. Am. Chem. Soc. 2013, 135, 15459−15466

solution is intimately mixed with the sample and frozen for the typical DNP experiment. For aqueous solutions this typically also requires the addition of a glass former such as glycerol or dimethyl sulfoxide (DMSO); without the glass former the DNP effect is usually absent. In dissolution DNP experiments the paramagnetic agent must be either ideally completely removed from the solution (within a few seconds) before it can be injected into an in vivo subject or at least reduced (for example, by addition of ascorbic acid),[38] to both prolong the lifetime of the solute polarization and to obtain high-resolution in vitro NMR spectra. Removal of OX063 can be achieved by precipitation via acidification of the solution followed by filtration.[39−41] Similarly, precipitation of the polarizing agents BDPA and DPPH has been demonstrated by Lumata et al.[42,43] However, efficient radical separation relies upon solubility differences between the radical and substrate and needs to be developed on a case by case basis for each radical/substrate/solvent set. While radical scavenging is an elegant and effective alternative,[38] it leaves the parent molecule of the radical in solution, as well as the scavenger (e.g., ascorbic acid), which may be undesirable in certain clinical applications.[38,39,44] Finally, the glass formers, which are not usually removed, may be metabolized themselves, which could perturb in vivo metabolic assays.[45]

Here we show how an insoluble hybrid organic−inorganic material containing homogeneously distributed radical that can be used as a polarization source for low-temperature DNP without the need for a glass former such as glycerol or DMSO. We establish the design principles for such a material, and we demonstrate polarization of substrates that impregnate the materials at ∼100 K. We show that ^{13}C-labeled pyruvate and alanine, examples of metabolic markers, are polarized efficiently with these materials. After dissolution, the polarizing matrix can easily be separated by filtration to yield a pure polarized liquid, containing only the solvent and the substrate (with no adjuvants). These materials have tremendous potential as a general polarization matrix for DNP. To illustrate the flexibility of this new platform for DNP, we show how a biradical bTUrea[37,46] that is poorly soluble (∼1 mM) in water in its molecular form can be incorporated into the material and used to polarize pure aqueous solutions.

Radical-containing materials have been investigated previously for DNP.[47−49] DNP signal enhancements of ∼120 were obtained for water in room temperature Overhauser DNP at low magnetic fields (<0.5 T) using a spin-labeled silica gel[50] or a thermoresponsive polymer.[51] To date there has been no effort to develop similar polarization matrixes for low-temperature DNP at high magnetic fields, which could yield much larger overall sensitivity enhancements. Spin-labeled silica materials have been studied with the objective of polarizing the surface of the materials themselves, but with disappointing results.[49] Here we show that specifically designed hybrid silica−organic materials can be used as low-temperature DNP polarization matrixes and that efficient DNP depends critically on obtaining a homogeneous distribution of the radicals, at an optimum concentration, inside the large pores of the mesostructured material.[52,53]

RESULTS AND DISCUSSION

Synthesis of Silica Materials Containing Regularly Distributed TEMPO Moieties. TEMPO-functionalized mesostructured hybrid silica materials (**Mat-TEMPO**) were prepared in a broad range of radical concentrations (0.010−0.28 mmol g^{-1}) according to the synthesis shown in Figure 1. The materials were prepared via sol−gel techniques in the presence of a structure-directing agent to control the size and the arrangement of the mesopores, the functional group density, and the distribution of organic groups within the pores of the silica material.[52,53] The choice of tetraethoxysilane (TEOS) as the diluent and (3-azidopropyl)trimethoxysilane as the apolar organic precursor[54,55] allows access to precursor materials (**Mat-Azide**) with a broad range of concentrations (here with (3-azidopropyl)trimethoxysilane/TEOS concentration ratios varying from 1/500 to 1/10), while maintaining the structure of the material with high surface areas (650−1050 m^2/g) and well-defined pore sizes (5.4−9.2 nm) (see the methods and Table S1 in the Supporting Information for details).

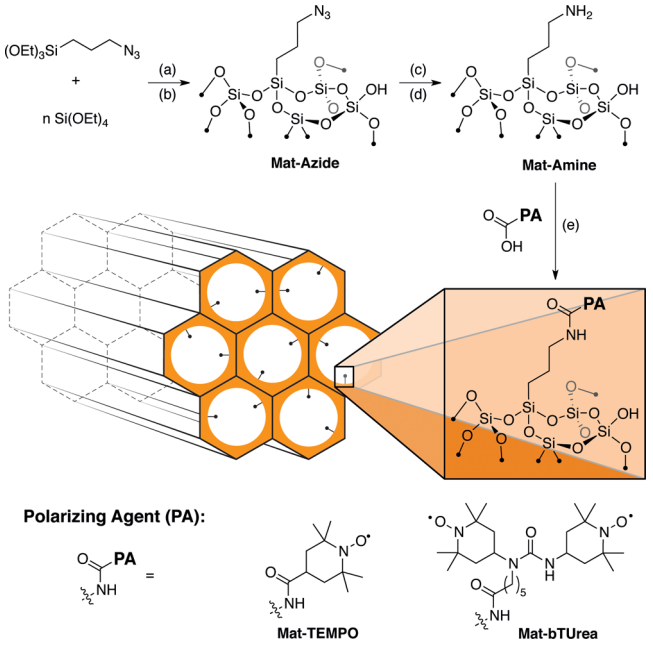

Figure 1. Synthesis of **Mat-TEMPO** and **Mat-bTUrea**. Reagents: (a) Pluronic P123, NaF, HCl(aq); (b) HCl(aq), pyridine; (c) PPhMe$_2$, THF; (d) H_2O; (e) HBTU, HOBt, DIPEA, THF, DMF. The synthesis is versatile and allows attachment of different polarizing agents (PAs) to the material. The ratio between the (3-azidopropyl)trimethoxysilane and TEOS ($1/n$) was varied to control the concentration of organic moieties in the material (see the Supporting Information for details); the name of the materials is thus referred to as $1/n$ **Mat-TEMPO** or $1/n$ **Mat-bTUrea**.

Mat-Azide materials in lower concentrations (1/34 to 1/500) afforded 2D hexagonal frameworks, while wormlike structures were obtained for higher concentrations (1/10 to 1/25) as evidenced by small-angle X-ray scattering (SAXS) and confirmed by transmission electron microscopy (TEM). The azido groups in **Mat-Azide** materials are readily converted into the corresponding amines (**Mat-Amine**) via the Staudinger reaction.[17] Hydroxybenzotriazole-mediated peptide coupling with 4-carboxy-TEMPO yields **Mat-TEMPO** (see the Supporting Information for details). Nitrogen adsorption and TEM examination of **Mat-Amine** and **Mat-TEMPO** materials established that the textural properties of **Mat-Azide** are largely conserved during these chemical transformations and result only in minor decreases of surface areas.

The radical content of the **Mat-TEMPO** materials was determined by continuous wave (CW) EPR spectroscopy at

dx.doi.org/10.1021/ja405822h | J. Am. Chem. Soc. 2013, 135, 15459−15466

room temperature. The radical concentration increases proportionally to the concentration of organic groups introduced in the material (Table S2, Figures S1 and S2, Supporting Information). The determined radical content indicates that conversion to **Mat-TEMPO** proceeds in 20−33% overall efficiency.

Measurement of DNP Enhancements for Frozen Solutions at 100 K. The polarizing efficiency of these materials was evaluated using a 400 MHz Bruker solid-state MAS DNP NMR instrument.[56] **Mat-TEMPO** materials were impregnated with $C_2H_2Cl_4$ or water,[29,57] loaded into a 3.2 mm sapphire rotor, and cooled to ca. 100 K, and NMR spectra (^{1}H, ^{13}C, and ^{29}Si) were recorded with or without microwave irradiation to determine the enhancement factors. The enhancements for ^{1}H (ε_H) and for ^{13}C and ^{29}Si under cross-polarization (CP) conditions ($\varepsilon_{C\ CP}$, and $\varepsilon_{Si\ CP}$, respectively) are shown in Figure 2, and the data are summarized in Tables S2 and S3 in the Supporting Information. The ε_H and $\varepsilon_{C\ CP}$ for $C_2H_2Cl_4$ were obtained from the solvent resonances and correspond to enhancement of solvent molecules within the pores of the material. The $\varepsilon_{Si\ CP}$ signal enhancement was obtained for the silicon resonance corresponding to the silicon atoms on the surface. Note that the hyperpolarization is transmitted via the proton polarization in these experiments; the silicon or the carbon nuclei were not directly polarized. The signal enhancement for materials wetted with $C_2H_2Cl_4$ increases from negligible enhancements of [ε_H, $\varepsilon_{C\ CP}$, $\varepsilon_{Si\ CP}$] = [1, 1, 2] for 1/500 **Mat-TEMPO** to maxima of [ε_H, $\varepsilon_{C\ CP}$, $\varepsilon_{Si\ CP}$] = [21, 21, 16] for 1/34 **Mat-TEMPO** before decreasing again at higher radical concentration. Similar behavior is observed for **Mat-TEMPO** impregnated with water, with an optimum for materials with dilutions of 1/34 and 1/25 with respective enhancements of [ε_H, $\varepsilon_{Si\ CP}$] = [22, 36] and [ε_H, $\varepsilon_{Si\ CP}$] = [17, 36].

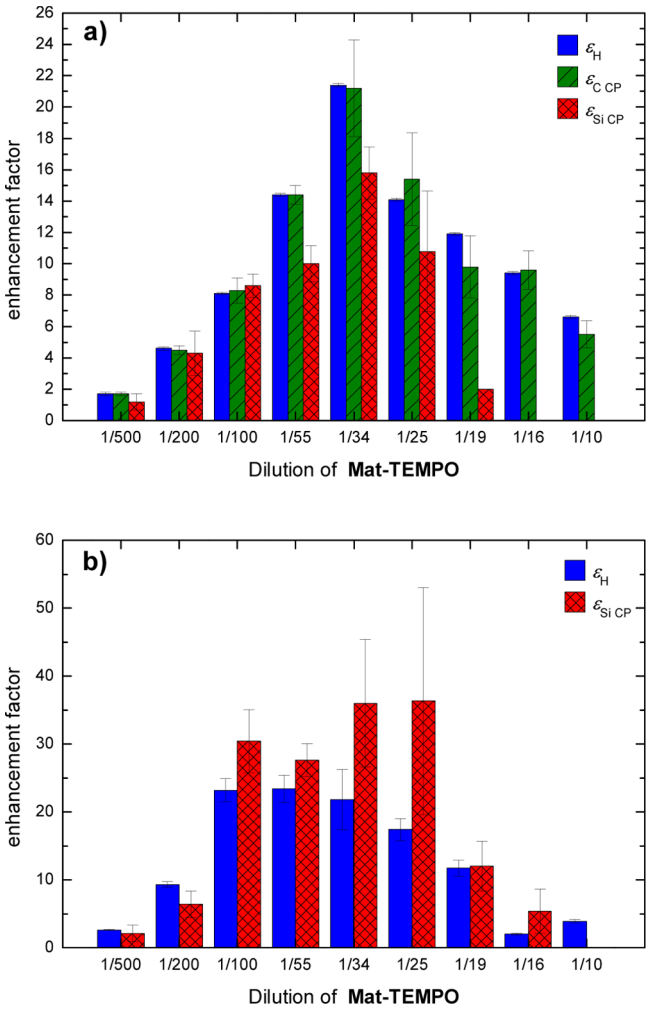

Figure 2. DNP enhancements as a function of the radical concentration and material dilution. (a) Enhancements of **Mat-TEMPO** impregnated with $C_2H_2Cl_4$. ε_H and $\varepsilon_{C\ CP}$ were obtained from the $C_2H_2Cl_4$ resonances, and $\varepsilon_{Si\ CP}$ was obtained from the bulk surface resonance. (b) **Mat-TEMPO** wetted with water. ε_H was measured from the resonance of water, and $\varepsilon_{Si\ CP}$ was obtained from the bulk silica surface signal.

Understanding the Influence of the Radical Concentration on DNP Enhancements. The radical concentration in **Mat-TEMPO** strongly affects DNP enhancements, as illustrated in Figure 2, with a trend similar to that typically observed for frozen solutions.[14,29] DNP enhancements are influenced by the radical concentration in two ways: (i) a higher concentration increases the overall rate of polarization flow from the electron to the proton spin bath, and (ii) the concentration controls the average inter-radical distance, which determines the average electron−electron dipolar coupling for monoradicals and influences electronic and nuclear relaxation properties. With regard to point ii, Griffin and co-workers have shown that, for the cross-effect, larger dipolar couplings (shorter interelectron distances) are likely to lead to higher DNP enhancements for biradical polarizing agents, at least down to the shortest mean distances that can be achieved in our materials.[14−16,18,37] Additionally, we have recently demonstrated that longer electron longitudinal relaxation times (T_{1e}) provide larger DNP enhancements.[17] Therefore, when the cross-effect is the dominant polarization transfer mechanism, the maximum DNP enhancement for monoradicals should occur at a compromise between radical concentrations where the dipolar couplings are largest and where the electronic relaxation times are not too short. This implies that the local concentration of radicals on the surface of polarizing matrixes, and thus the radical distribution within the material, will have a strong effect on the DNP efficiency. For high radical concentrations (1/10 to 1/100 **Mat-TEMPO**, corresponding to concentrations greater than 0.038 mmol g^{-1}) the average inter-radical distance can be directly probed by the peak-to-peak line width in the EPR spectra, as strong electron dipolar coupling and/or spin exchange lead to broadening of the signal.[58] Figure 3a shows the results of X-band (9.5 GHz) EPR line width analysis relative to the radical concentration in the material and the correlation of the EPR line width with measured DNP ^{1}H enhancements. The measured EPR line width varies from 11.7 G (1/500) to 21.1 G (1/10) for **Mat-TEMPO** as the concentration varies from 0.010 to 0.28 mmol of radical g^{-1} (Figure 3a; Table S4, Supporting Information).

Electron relaxation properties are also influenced by the average inter-radical separation due to spin exchange and dipolar coupling. The electron T_{1e} was measured by inversion recovery experiments on solvent-impregnated **Mat-TEMPO** at 105 K. The signal buildups were fitted to stretched exponential functions [$S(t) = S_0(1 - \exp(-(t/T_{1e}{}^*)^\beta))$]. We characterize electron relaxation by $\langle T_{1e} \rangle$, which is the first moment of the distribution and describes a mean recovery time (Figure 3b; Table S4, Supporting Information). Discussion in terms of a mean relaxation time rather than a mean relaxation rate is

dx.doi.org/10.1021/ja405822h | J. Am. Chem. Soc. 2013, 135, 15459−15466

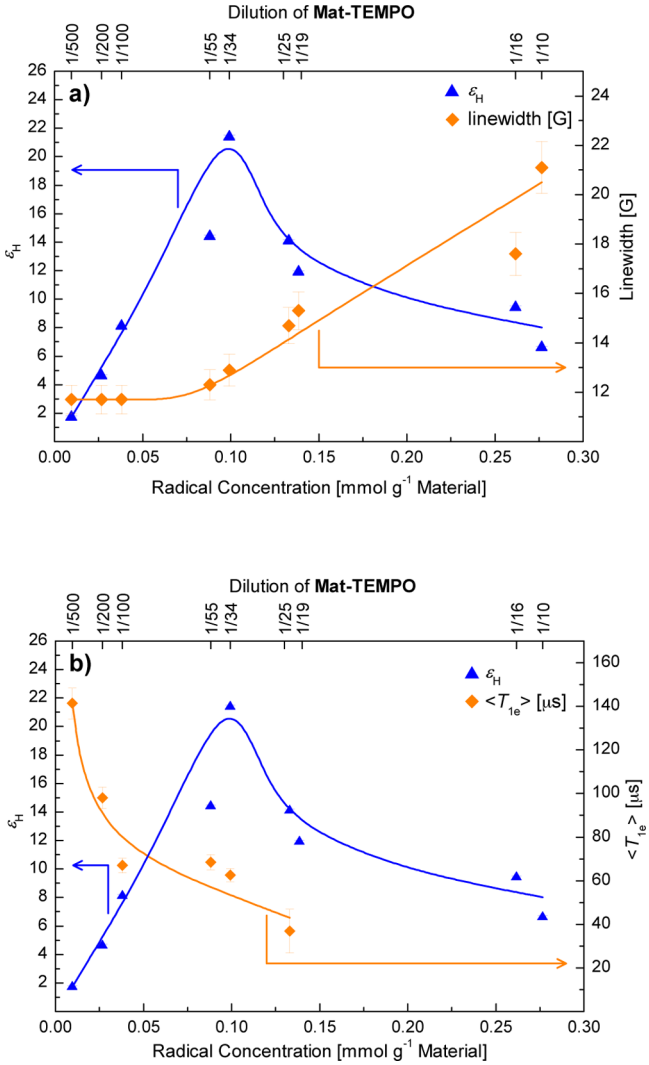

Figure 3. X-band EPR line width (a) and mean electron recovery time (b) plotted versus the radical concentration in **Mat-TEMPO**. ε_H (^{1}H DNP enhancement factor) as a function of the radical concentration in **Mat-TEMPO** materials wetted with $C_2H_2Cl_4$ is also in (a) and (b). The lines passing through the points are for visual aid only. The arrows present in (a) and (b) indicate the respective axis. $\langle T_{1e}\rangle$ is not presented for the highest radical concentrations because no detectable echo could be observed by pulsed EPR.

permitted if only trends are evaluated (but since here the measurement is not in any case done at the same field as the DNP experiments, the measurements are only intended to demonstrate trends). Note also that, at the radical concentrations used here, which are relevant to the DNP experiments, the recovery time does not correspond to the "intrinsic" T_{1e} and will be affected by spin diffusion. However, the recovery times measured here are the most relevant to the DNP process. $\langle T_{1e}\rangle$ decreases substantially with increasing radical concentration for **Mat-TEMPO** within the range of 1/25 to 1/500 (Figure 3b), demonstrating the sensitivity to inter-radical distances. Therefore, it is clear that the observation of an optimum radical concentration for DNP arises due to the interplay between increased electron dipolar coupling and a reduction in the effective electron relaxation times, consistent with the hypotheses above.

Optimum DNP Enhancements from Proper Radical Distributions in the Materials. As discussed above, the DNP enhancement will depend upon the distribution of radicals within the pores of the material. The ideal material would show an absolutely regular distribution with a single inter-radical distance ($\langle R_{ee}\rangle$). Hence, the method used for synthesis of these materials is expected to strongly impact the attainable DNP enhancement. The direct synthesis via sol–gel condensation in the presence of a structure-directing template used in this study is expected to generate materials with a statistical distribution on the two-dimensional surface, therefore precluding aggregation of the radicals. To illustrate this key feature, we compared the DNP enhancements and EPR spectra for **Mat-TEMPO** and materials prepared by postgrafting onto an unfunctionalized mesoporous silica material.

In stark contrast to **Mat-TEMPO**, materials prepared by postgrafting of the organic groups onto presynthetized silica material (see the Supporting Information for experimental details) provide poor DNP enhancements. For example, SBA-type silica[59] functionalized via postgrafting had a radical concentration of 0.14 mmol g^{-1}, which is directly comparable with that of **Mat-TEMPO** 1/19. The grafted radical material exhibited a much broader EPR line width (27.0 vs 15.3 G for **Mat-TEMPO** 1/19; Figure S3, Supporting Information), and consequently inferior DNP enhancements were obtained for this material (ε_H = 2). This strongly suggests that postgrafting leads to an inhomogeneous distribution of TEMPO groups on the surface, leading to high local radical concentrations and poor DNP. We also investigated SilicaCat, a commercially available silica material with TEMPO linked by an amine propyl chain to a silica surface that contains 0.47 mmol of radical g^{-1}. This material also had a very broad EPR signal (26.5 G, Figure S3), and the DNP enhancement is low (ε_H = 4). These results establish that the regular placement of the radical in the material is essential for efficient NMR signal enhancements.

Furthermore, we can compare the enhancements observed for materials with radicals bound to the pore surface to those observed for materials impregnated with a TEMPO solution. We prepared a sample of **Mat-PhOH**, a related mesoporous material that contains DNP inert phenol groups in place of TEMPO moieties as the sole organic component,[60] with a 80 mM solution of TEMPO in $C_2H_2Cl_4$, which corresponds to 0.12 mmol of radical g^{-1}. The DNP enhancements of this material were [ε_H, $\varepsilon_{C\ CP}$, $\varepsilon_{Si\ CP}$] = [14, 15, 8]. The $C_2H_2Cl_4$-impregnated 1/34 **Mat-TEMPO** material contains a radical loading (0.10 mmol of radical g^{-1}) similar to that of **Mat-PhOH** wetted with TEMPO and gives DNP enhancements of [ε_H, $\varepsilon_{C\ CP}$, $\varepsilon_{Si\ CP}$] = [21, 21, 16]. We should note that these two material conditions were chosen because the best signal enhancements were obtained for 1/34 **Mat-TEMPO** in the radical-containing material class, and in the case of **Mat-PhOH** the optimal wetting conditions were with 80 mM TEMPO in $C_2H_2Cl_4$. The EPR line width of the 1/34 **Mat-TEMPO** is 12.9 G, and that of **Mat-PhOH** wetted with 80 mM TEMPO solution is 14.9 G (see Tables S4 and S5, Supporting Information). In agreement with the line width analysis, a much shorter $\langle T_{1e}\rangle$ was found for the radicals in the wetted **Mat-PhOH** than for the radicals in **Mat-TEMPO** (see Table S5).

The EPR line widths of **Mat-PhOH** impregnated with 20–120 mM TEMPO solutions in $C_2H_2Cl_4$ were, in all cases, broader than the EPR line widths of pure TEMPO solutions (20–100 mM) and more importantly of **Mat-TEMPO** materials with a comparable amount of radical inside the material (1/100 to 1/10; Tables S4 and S5, Supporting

dx.doi.org/10.1021/ja405822h | J. Am. Chem. Soc. 2013, 135, 15459–15466

Information). This result indicates that **Mat-PhOH** impregnated with 20−120 mM TEMPO/$C_2H_2Cl_4$ solutions contain local aggregates of radicals that result in lower overall DNP enhancement. For **Mat-TEMPO** materials, this aggregation is prohibited by covalent attachment of the functional group to the surface, and thus, the inter-radical separation is on average greater and more uniform than in materials wetted with exogenous radical solutions. This leads to larger DNP enhancements than obtained for impregnated materials.

With these insights in hand, we sought to correlate the average inter-radical distance ($\langle R_{ee} \rangle$) with DNP enhancements. We modeled the radicals in the material as a homogeneous random distribution along the surface of the pore channel to determine a pair distribution function for the radicals (Figure S4, Table S6, Supporting Information). The simulated EPR spectra, using the simplifying assumption that spectral line broadening only occurs via dipolar interactions between two radicals, reproduce surprisingly well the experiments for **Mat-TEMPO** materials for concentrations up to 0.10 mmol g^{-1} (Table S6). The simulated and experimental line widths differ by less than 1% for materials up to 0.10 mmol rad^{-1}, clearly supporting the idea of a homogeneous distribution of radicals along the pore channel (Figure S5, Table S6). Above 0.10 mmol g^{-1}, the line width of the experimental spectrum becomes significantly broader than the simulation, but this deviation is probably due to broadening through other mechanisms, such as spin exchange or transverse relaxation time, at higher concentrations that were not considered in the model.[61,62]

In solid-state DNP at 100 K and high fields, the most efficient mechanism for nuclear spin polarization is the cross-effect, requiring the radicals interact via dipolar coupling.[37] Rigid biradicals with fixed relative orientations and inter-radical distances exploit the cross-effect to deliver maximum enhancements in DNP.[14] For example, the biradicals bTbK and bCTbK,[16,17] which give far greater DNP enhancements than flexible biradicals, have an average inter-radical distance close to 1.2 nm. Assuming this is an optimal distance between radicals, the fraction of radicals in the 1.2−1.4 nm range was calculated from the model and is given in Table S6 (Supporting Information) for the different materials. At the high radical concentrations the population of radicals approximately 1.3 nm apart actually remains more or less constant over the range from 1/10 to 1/34 (from 0.28 to 0.10 mmol g^{-1}). However, at these concentrations, a large fraction of the radicals are separated by shorter distances. The shorter inter-radical distances lead to broadening of the EPR lines and shorter T_{1e}, and hence, we predict a relative loss of signal enhancement for the higher concentrations. At lower radical concentrations (1/55 to 1/500), the fraction with the optimum inter-radical distance decreases continuously, which is also consistent with the drop in DNP enhancements at low concentrations.

These predictions support the experimentally observed optimal radical concentration found in **Mat-TEMPO** 1/34. This material possesses a large proportion of radicals at appropriate inter-radical distances, yet this material is relatively devoid of short $\langle R_{ee} \rangle$, leading to a sufficiently long T_{1e}.

This analysis highlights the critical importance of controlling inter-radical distances in polarizing matrixes to obtain good DNP enhancements.

Mat-TEMPO Materials as Efficient Polarizing Matrixes. The applicability of the materials as polarizing matrixes for molecules in solution was evaluated using aqueous solutions of

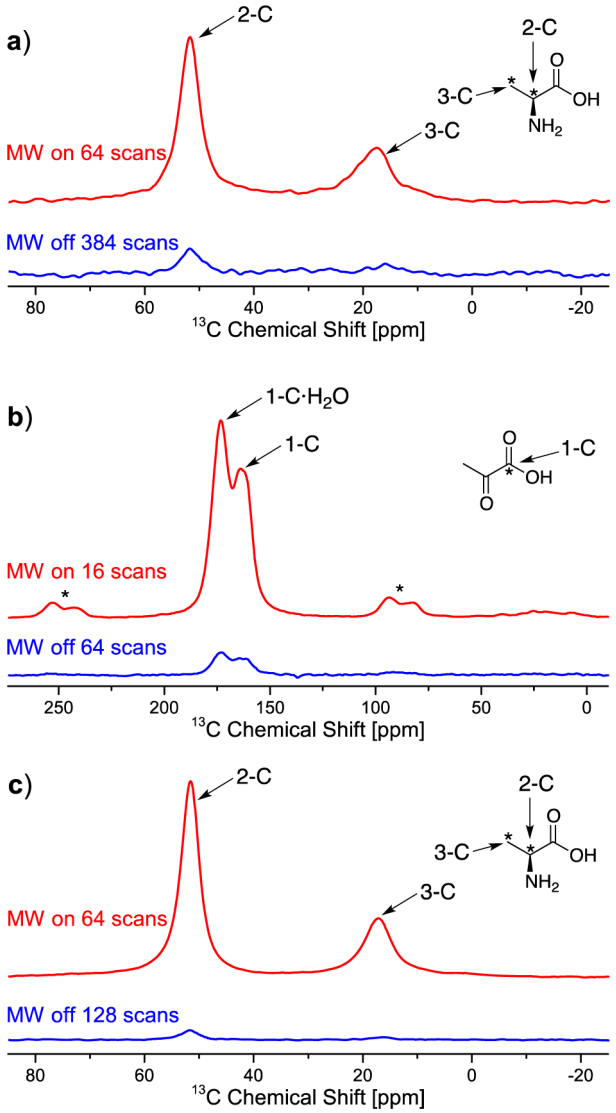

Figure 4. ^{13}C CP MAS NMR spectra of (a) [2,3-^{13}C]-L-alanine and (b) [1-^{13}C]pyruvic acid both enhanced by 1/34 **Mat-TEMPO** and (c) [2,3-^{13}C]-L-alanine enhanced by 1/100 **Mat-bTUrea**. In all three cases, the probe molecule was dissolved in pure H_2O. The microwave on spectrum is presented in red, and the microwave off spectrum is in blue. In (a) $\varepsilon_{C\ CP}$ was 39, in (b) $\varepsilon_{C\ CP}$ was 34, and in (c) $\varepsilon_{C\ CP}$ was 45. The unlabeled carbons in these samples were not detected. In (b), the two 1-C resonances correspond to the keto acid and the 2-hydrated pyruvic acid ($MeC(OH)_2COOH$).

[2,3-^{13}C]-L-alanine or [1-^{13}C]pyruvic acid dissolved in water (Figure 4). In this context the compounds serve as examples of potential labeled metabolic tracers for in vivo applications.[63] Only 20 μL of either a 0.1 M solution of [2,3-^{13}C]-L-alanine or a 0.5 M solution of [1-^{13}C]pyruvic acid was used to impregnate small quantities of 1/34 **Mat-TEMPO** (13 mg), the optimal material for DNP enhancement. The ^{13}C CPMAS spectra of [2,3-^{13}C]-L-alanine or [1-^{13}C]pyruvic acid wetted 1/34 **Mat-TEMPO** are shown in Figure 4. $\varepsilon_{C\ CP}$ = 39 for the labeled alanine resonances, and $\varepsilon_{C\ CP}$ = 34 for labeled pyruvic acid. Both of these values are similar to those obtained from solvent signal enhancements presented above. Note that, in the ^{13}C CPMAS spectrum of pyruvic acid, the two observed resonances are assigned to the keto and the hydrated acid.[64−66]

dx.doi.org/10.1021/ja405822h | J. Am. Chem. Soc. 2013, 135, 15459−15466

These results clearly show that significant signal enhancements of analyte molecules in frozen solutions can be achieved using **Mat-TEMPO** materials at 100 K. Of course, polarization of solutions for in vivo applications of dissolution DNP are usually carried out at much lower temperatures than available here (and do not involve magic angle spinning). However, there is no reason to presume that the performance of the materials would be significantly compromised at low temperature, and by extrapolation, we therefore expect polarization of several tens of percent at liquid helium temperatures. Such experiments will be described in a future paper.

Separation of the substrate in solution from the polarizing matrix can be achieved via simple filtration and washing of the **Mat-TEMPO** with the solvent used in the experiment. For a representative example, **Mat-TEMPO** (10 mg, 1 μmol, of radical), previously washed with ethanol, was wetted with 16 μL of an aqueous solution containing 8 μmol of pyruvic acid. The pyruvic acid was quantitatively recovered by simply washing the material with 500 μL of water (>93%). Determination of the radical content in this solution revealed that only negligibly small quantities of radical (ca. 0.5 nmol, less than 0.1% of the radical present in the material) leach during contact with the analyte solution. Experiments with *m*-xylene as the analyte and $C_2H_2Cl_4$ as the solvent yielded quantitative recovery of xylene and showed no evidence of radical leaching according to EPR (<0.01 nmol).

Insoluble Biradicals To Polarize Aqueous Solutions. These materials in fact provide a very versatile platform for polarization. For example, there is currently much activity directed to designing more efficient radicals, and the best radicals for cross-effect DNP are currently water-insoluble systems such as bCTbK.[17,67] Rendering such systems water-soluble involves substantial synthetic manipulations.[19,68] Here, however, with this material scaffold incorporation of insoluble radicals is straightforward. The radical concentrations required for DNP will not significantly affect the hydrophobicity of the materials, and they would maintain water compatibility. In effect, this material-centered approach allows the design of new polarizing radicals that are no longer determined solely by solubility.

As an example, we have incorporated bTUrea[37,46] to form **Mat-bTUrea** (Figure 1) in three representative concentrations: 1/34, 1/100, and 1/200 (see the Supporting Information for details on the synthesis and characterization). We expect lower concentrations of biradical to be more effective as compared to **Mat-TEMPO**, and we obtain an enhancement of $\varepsilon_{C\ CP} = 45$ for [2,3-^{13}C]-L-alanine with a **Mat-bTUrea** 1/100 polarizing matrix, which gave a higher enhancement than the 1/34 or 1/200 material, as illustrated in Figure 4. These radicals could otherwise not be used to polarize aqueous solutions. The overall efficiency of these materials-based systems is very comparable to that of bulk alternatives (for example, 10 mM TOTAPOL typically produces $\varepsilon \approx 40$ at 9.4 T and 100 K in DMSO-d_6/D_2O/H_2O (60/30/10)).

CONCLUSION

Hybrid silica mesostructured materials containing homogeneously distributed mono- or dinitroxide functional groups provide efficient solid-phase DNP matrixes. The high performance of these materials results from rigorous design elements for efficient polarization transfer. The homogeneous distribution of radical moieties within the porous network of the materials is essential to prevent unwanted radical aggregation that can occur by postsynthetic grafting strategies. The homogeneity of the radical distribution in **Mat-TEMPO** materials yields optimal distributions of radicals and inter-radical distances that are best for the cross-effect. Delicately balancing competing effects on the DNP process here yields high-performance materials that efficiently polarize solvents and small molecules. These experiments are particularly promising because in principle almost any metabolic marker could be polarized using this solid matrix. After thawing, the separation of the matrix from the solution is straightforward and leaves a pure polarized solution suitable for in vivo studies without any need for chemical treatment and without undesired byproducts. Furthermore, the material provides a highly versatile platform that can be extended to biradicals for improved cross-effect DNP, as demonstrated here by the incorporation of the otherwise insoluble radical bTUrea, which is then used to polarize aqueous solutions or to narrow line radicals such as OX063 for liquid helium temperature dissolution DNP. These applications are currently under investigation in our laboratories.

ASSOCIATED CONTENT

Supporting Information

Experimental procedures and details, additional data, Figures S1−S5, and Tables S1−S8. This material is available free of charge via the Internet at http://pubs.acs.org.

AUTHOR INFORMATION

Corresponding Authors

chloe.thieuleux@univ-lyon1.fr
lyndon.emsley@ens-lyon.fr
ccoperet@ethz.ch

Author Contributions

⊥D.G. and M.S. contributed equally to this work.

Notes

The authors declare no competing financial interest.

ACKNOWLEDGMENTS

We thank Bruker (Drs. Marc Caporini, Melanie Rosay, Werner Maas, and Alain Belguise) for providing access to the solid-state DNP spectrometer. We acknowledge financial support from EQUIPEX Contract ANR-10-EQPX-47-01, SNF Project Number 200021_134775/1, ERC Advanced Grant No. 320860, and the ETH Zürich. A.J.R. acknowledges the European Union for a Marie Curie fellowship (Grant PIIF-GA-2010-274574).

REFERENCES

(1) Overhauser, A. W. *Phys. Rev.* **1953**, *92*, 411.
(2) Carver, T. R.; Slichter, C. P. *Phys. Rev.* **1953**, *92*, 212.
(3) Ardenkjaer-Larsen, J. H.; Fridlund, B.; Gram, A.; Hansson, G.; Hansson, L.; Lerche, M. H.; Servin, R.; Thaning, M.; Golman, K. *Proc. Natl. Acad. Sci. U.S.A.* **2003**, *100*, 10158.
(4) Day, S. E.; Kettunen, M. I.; Gallagher, F. A.; Hu, D. E.; Lerche, M.; Wolber, J.; Golman, K.; Ardenkjaer-Larsen, J. H.; Brindle, K. M. *Nat. Med.* **2007**, *13*, 1382.
(5) Frydman, L.; Blazina, D. *Nat. Phys.* **2007**, *3*, 415.
(6) Gallagher, F. A.; Kettunen, M. I.; Day, S. E.; Hu, D. E.; Ardenkjaer-Larsen, J. H.; in't Zandt, R.; Jensen, P. R.; Karlsson, M.; Golman, K.; Lerche, M. H.; Brindle, K. M. *Nature* **2008**, *453*, 940.
(7) Keshari, K. R.; Wilson, D. M.; Chen, A. P.; Bok, R.; Larson, P. E. Z.; Hu, S.; Van Criekinge, M.; Macdonald, J. M.; Vigneron, D. B.; Kurhanewicz, J. *J. Am. Chem. Soc.* **2009**, *131*, 17591.

(8) Harris, T.; Eliyahu, G.; Frydman, L.; Degani, H. *Proc. Natl. Acad. Sci. U.S.A.* **2009**, *106*, 18131.
(9) Gallagher, F. A.; Kettunen, M. I.; Brindle, K. M. *Prog. Nucl. Magn. Reson. Spectrosc.* **2009**, *55*, 285.
(10) Schroeder, M. A.; Atherton, H. J.; Cochlin, L. E.; Clarke, K.; Radda, G. K.; Tyler, D. J. *Magn. Reson. Med.* **2009**, *61*, 1007.
(11) Keshari, K. R.; Kurhanewicz, J.; Bok, R.; Larson, P. E. Z.; Vigneron, D. B.; Wilson, D. M. *Proc. Natl. Acad. Sci. U.S.A.* **2011**, *108*, 18606.
(12) Merritt, M. E.; Harrison, C.; Sherry, A. D.; Malloy, C. R.; Burgess, S. C. *Proc. Natl. Acad. Sci. U.S.A.* **2011**, *108*, 19084.
(13) Clatworthy, M. R.; Kettunen, M. I.; Hu, D. E.; Mathews, R. J.; Witney, T. H.; Kennedy, B. W. C.; Bohndiek, S. E.; Gallagher, F. A.; Jarvis, L. B.; Smith, K. G. C.; Brindle, K. M. *Proc. Natl. Acad. Sci. U.S.A.* **2012**, *109*, 13374.
(14) Hu, K.-N.; Yu, H.-h.; Swager, T. M.; Griffin, R. G. *J. Am. Chem. Soc.* **2004**, *126*, 10844.
(15) Song, C.; Hu, K.-N.; Joo, C.-G.; Swager, T. M.; Griffin, R. G. *J. Am. Chem. Soc.* **2006**, *128*, 11385.
(16) Matsuki, Y.; Maly, T.; Ouari, O.; Karoui, H.; Le Moigne, F.; Rizzato, E.; Lyubenova, S.; Herzfeld, J.; Prisner, T.; Tordo, P.; Griffin, R. G. *Angew. Chem., Int. Ed.* **2009**, *48*, 4996.
(17) Zagdoun, A.; Casano, G.; Ouari, O.; Lapadula, G.; Rossini, A. J.; Lelli, M.; Baffert, M.; Gajan, D.; Veyre, L.; Maas, W. E.; Rosay, M.; Weber, R. T.; Thieuleux, C.; Coperet, C.; Lesage, A.; Tordo, P.; Emsley, L. *J. Am. Chem. Soc.* **2012**, *134*, 2284.
(18) Dane, E. L.; Corzilius, B.; Rizzato, E.; Stocker, P.; Maly, T.; Smith, A. A.; Griffin, R. G.; Ouari, O.; Tordo, P.; Swager, T. M. *J. Org. Chem.* **2012**, *77*, 1789.
(19) Kiesewetter, M. K.; Corzilius, B. r.; Smith, A. A.; Griffin, R. G.; Swager, T. M. *J. Am. Chem. Soc.* **2012**, *134*, 4537.
(20) Hall, D. A.; Maus, D. C.; Gerfen, G. J.; Inati, S. J.; Becerra, L. R.; Dahlquist, F. W.; Griffin, R. G. *Science* **1997**, *276*, 930.
(21) Bajaj, V. S.; Mak-Jurkauskas, M. L.; Belenky, M.; Herzfeld, J.; Griffin, R. G. *Proc. Natl. Acad. Sci. U.S.A.* **2009**, *106*, 9244.
(22) Salnikov, E.; Rosay, M.; Pawsey, S.; Ouari, O.; Tordo, P.; Bechinger, B. *J. Am. Chem. Soc.* **2010**, *132*, 5940.
(23) Akbey, Ü.; Franks, W. T.; Linden, A.; Lange, S.; Griffin, R. G.; van Rossum, B.-J.; Oschkinat, H. *Angew. Chem., Int. Ed.* **2010**, *49*, 7803.
(24) Reggie, L.; Lopez, J. J.; Collinson, I.; Glaubitz, C.; Lorch, M. *J. Am. Chem. Soc.* **2011**, *133*, 19084.
(25) Linden, A. H.; Lange, S.; Franks, W. T.; Akbey, Ü.; Specker, E.; van Rossum, B.-J.; Oschkinat, H. *J. Am. Chem. Soc.* **2011**, *133*, 19266.
(26) Sergeyev, I. V.; Day, L. A.; Goldbourt, A.; McDermott, A. E. *J. Am. Chem. Soc.* **2011**, *133*, 20208.
(27) Jacso, T.; Franks, W. T.; Rose, H.; Fink, U.; Broecker, J.; Keller, S.; Oschkinat, H.; Reif, B. *Angew. Chem., Int. Ed.* **2012**, *51*, 432.
(28) Renault, M.; Pawsey, S.; Bos, M. P.; Koers, E. J.; Nand, D.; Tommassen-van Boxtel, R.; Rosay, M.; Tommassen, J.; Maas, W. E.; Baldus, M. *Angew. Chem., Int. Ed.* **2012**, *51*, 2998.
(29) Lesage, A.; Lelli, M.; Gajan, D.; Caporini, M. A.; Vitzthum, V.; Miéville, P.; Alauzun, J.; Roussey, A.; Thieuleux, C.; Mehdi, A.; Bodenhausen, G.; Coperet, C.; Emsley, L. *J. Am. Chem. Soc.* **2010**, *132*, 15459.
(30) Lelli, M.; Gajan, D.; Lesage, A.; Caporini, M. A.; Vitzthum, V.; Miéville, P.; Heroguel, F.; Rascon, F.; Roussey, A.; Thieuleux, C.; Boualleg, M.; Veyre, L.; Bodenhausen, G.; Coperet, C.; Emsley, L. *J. Am. Chem. Soc.* **2011**, *133*, 2104.
(31) Rossini, A. J.; Zagdoun, A.; Lelli, M.; Canivet, J.; Aguado, S.; Ouari, O.; Tordo, P.; Rosay, M.; Maas, W. E.; Copéret, C.; Farrusseng, D.; Emsley, L.; Lesage, A. *Angew. Chem., Int. Ed.* **2011**, 123.
(32) Vitzthum, V.; Mieville, P.; Carnevale, D.; Caporini, M. A.; Gajan, D.; Copéret, C.; Lelli, M.; Zagdoun, A.; Rossini, A. J.; Lesage, A.; Emsley, L.; Bodenhausen, G. *Chem. Commun.* **2012**, *48*, 1988.
(33) Rossini, A. J.; Zagdoun, A.; Lelli, M.; Lesage, A.; Copéret, C.; Emsley, L. *Acc. Chem. Res.* **2013**, *46*, 1942−1951.
(34) Rossini, A. J.; Zagdoun, A.; Hegner, F.; Schwarzwälder, M.; Gajan, D.; Copéret, C.; Lesage, A.; Emsley, L. *J. Am. Chem. Soc.* **2012**, *134*, 16899.
(35) Ardenkjaer-Larsen, J. H.; Macholl, S.; Johannesson, H. *Appl. Magn. Reson.* **2008**, *34*, 509.
(36) Sze, K. H.; Wu, Q.; Tse, H. S.; Zhu, G. *Top. Curr. Chem.* **2012**, *326*, 215.
(37) Hu, K. N.; Song, C.; Yu, H. H.; Swager, T. M.; Griffin, R. G. *J. Chem. Phys.* **2008**, *128*, 052302.
(38) Miéville, P.; Ahuja, P.; Sarkar, R.; Jannin, S.; Vasos, P. R.; Gerber-Lemaire, S.; Mishkovsky, M.; Comment, A.; Gruetter, R.; Ouari, O.; Tordo, P.; Bodenhausen, G. *Angew. Chem., Int. Ed.* **2010**, *49*, 6182.
(39) Ardenkjaer-Larsen, J. H.; Leach, A. M.; Clarke, N.; Urbahn, J.; Anderson, D.; Skloss, T. W. *NMR Biomed.* **2011**, *24*, 927.
(40) Harris, T.; Bretschneider, C.; Frydman, L. *J. Magn. Reson.* **2011**, *211*, 96.
(41) Leach, A. M.; Miller, P.; Telfeyan, E.; Whitt, D. B. (General Electric Co.). US2009263325-A1, 2009.
(42) Lumata, L.; Merritt, M.; Khemtong, C.; Ratnakar, S. J.; van Tol, J.; Yu, L.; Song, L.; Kovacs, Z. *RSC Adv.* **2012**, *2*, 12812.
(43) Lumata, L.; Ratnakar, S. J.; Jindal, A.; Merritt, M.; Comment, A.; Malloy, C.; Sherry, A. D.; Kovacs, Z. *Chem.—Eur. J.* **2011**, *17*, 10825.
(44) Lumata, L.; Merritt, M. E.; Malloy, C. R.; Sherry, A. D.; Kovacs, Z. *J. Phys. Chem. A* **2012**, *116*, 5129.
(45) Morozova, O.; Kaptein, R.; Sagdeev, R.; Yurkovskaya, A. *Appl. Magn. Reson.* **2013**, *44*, 233.
(46) Rozantsev, E. G.; Golubev, V. A.; Neiman, M. B.; Kokhanov, Y. V. *Izv. Akad. Nauk SSSR* **1965**, *3*, 572.
(47) McCarney, E. R.; Han, S. *J. Magn. Reson.* **2008**, *190*, 307.
(48) Vitzthum, V.; Borcard, F.; Jannin, S.; Morin, M.; Mieville, P.; Caporini, M. A.; Sienkiewicz, A.; Gerber-Lemaire, S.; Bodenhausen, G. *ChemPhysChem* **2011**, *12*, 2929.
(49) Thankamony, A. S. L.; Lafon, O.; Lu, X.; Aussenac, F.; Rosay, M.; Trebosc, J.; Vezin, H.; Amoureux, J.-P. *Appl. Magn. Reson.* **2012**, *43*, 237.
(50) Gitti, R.; Wild, C.; Tsiao, C.; Zimmer, K.; Glass, T. E.; Dorn, H. C. *J. Am. Chem. Soc.* **1988**, *110*, 2294.
(51) Dollmann, B. C.; Junk, M. J. N.; Drechsler, M.; Spiess, H. W.; Hinderberger, D.; Munnemann, K. *Phys. Chem. Chem. Phys.* **2010**, *12*, 5879.
(52) Corriu, R. J. P.; Mehdi, A.; Reye, C. *J. Mater. Chem.* **2005**, *15*, 4285.
(53) Hoffmann, F.; Cornelius, M.; Morell, J.; Fröba, M. *Angew. Chem., Int. Ed.* **2006**, *45*, 3216.
(54) Nakazawa, J.; Stack, T. D. P. *J. Am. Chem. Soc.* **2008**, *130*, 14360.
(55) Nakazawa, J.; Smith, B. J.; Stack, T. D. P. *J. Am. Chem. Soc.* **2012**, *134*, 2750.
(56) Rosay, M.; Tometich, L.; Pawsey, S.; Bader, R.; Schauwecker, R.; Blank, M.; Borchard, P. M.; Cauffman, S. R.; Felch, K. L.; Weber, R. T.; Temkin, R. J.; Griffin, R. G.; Maas, W. E. *Phys. Chem. Chem. Phys.* **2010**, *12*, 5850.
(57) Zagdoun, A.; Rossini, A. J.; Gajan, D.; Bourdolle, A.; Ouari, O.; Rosay, M.; Maas, W. E.; Tordo, P.; Lelli, M.; Emsley, L.; Lesage, A.; Coperet, C. *Chem. Commun.* **2012**, *48*, 654.
(58) Jeschke, G. *ChemPhysChem* **2002**, *3*, 927.
(59) Firouzi, A.; Kumar, D.; Bull, L. M.; Besier, T.; Sieger, P.; Huo, Q.; Walker, S. A.; Zasadzinski, J. A.; Glinka, C.; Nicol, J.; Margolese, D.; Stucky, G. D.; Chmelka, B. F. *Science* **1995**, *267*, 1138.
(60) Roussey, A.; Gajan, D.; Maishal, T. K.; Mukerjee, A.; Veyre, L.; Lesage, A.; Emsley, L.; Coperet, C.; Thieuleux, C. *Phys. Chem. Chem. Phys.* **2011**, *13*, 4230.
(61) Mims, W. B.; Nassau, K.; McGee, J. D. *Phys. Rev.* **1961**, *123*, 2059.
(62) Klauder, J. R.; Anderson, P. W. *Phys. Rev.* **1962**, *125*, 912.
(63) Lerche, M. H.; Meier, S.; Jensen, P. R.; Hustvedt, S.-O.; Karlsson, M.; Duus, J. O.; Ardenkjaer-Larsen, J. H. *NMR Biomed.* **2011**, *24*, 96.
(64) Hellstrom, N.; Almqvist, S.-O. *J. Chem. Soc. B* **1970**, 1396.

(65) Margolis, S. A.; Coxon, B. *Anal. Chem.* **1986**, *58*, 2504.
(66) Maron, M. K.; Takahashi, K.; Shoemaker, R. K.; Vaida, V. *Chem. Phys. Lett.* **2011**, *513*, 184.
(67) Ysacco, C. d.; Karoui, H.; Casano, G.; Moigne, F. o.; Combes, S. b.; Rockenbauer, A.; Rosay, M.; Maas, W.; Ouari, O.; Tordo, P. *Appl. Magn. Reson.* **2012**, *43*, 251.
(68) Haze, O.; Corzilius, B.; Smith, A. A.; Griffin, R. G.; Swager, T. M. *J. Am. Chem. Soc.* **2012**, *134*, 14287.